Comparison of the Vorticity of Acoustic Intensity Vector at 23 Hz and 110 Hz Frequencies in the Shallow Sea

Vladimir Shchurov

V.I.Il'ichev Pacific Oceanological Institute Far Eastern Branch of Russian Academy of Sciences

43, Baltiyskaya St., Vladivostok, 690041, Russia

Tel: 7-423-231-2101 E-mail: Shchurov@poi.dvo.ru

Received: July 21, 2011 Accepted: August 9, 2011 Published: November 1, 2011

doi:10.5539/apr.v3n2p179 URL: http://dx.doi.org/10.5539/apr.v3n2p179

The research was conducted with financial support from Russian –- Chinese grant RFFI_a no. 08-05-92210 – GFEN and the Federal Target Program "Science and science - teaching personnel of innovative Russia" (Federal Contract 14.740.11.0139).

Abstract

This paper presents the results of vortex features research of the field of acoustic intensity vector depending on distance and frequency by the combined acoustic systems in Peter the Great Bay (Sea of Japan). The receiver was submerged to 70 m depth at the site depth of 120 m, sound velocity on the surface was higher than that of the bottom's one. To determine the vorticity three components of curl of intensity vector were calculated. The work provides the distribution histograms of probability density in the normalized components of intensity vector curl at 110 Hz and 23 Hz frequencies for the distances interval between source and receiver within 1200 – 2000 m. The vortex structure of acoustic intensity vector was discovered in vertical plane along the entire researched distance (5000 m) between source and receiver. The described mechanism of acoustic energy transfer reveals new opportunities in the study of acoustic characteristics of the shallow sea. The disclosed vortex structures are of interest both for physical acoustics and for applied problems in underwater acoustics.

Keywords: Acoustic vortices, Acoustic intensity vector, Vectorial acoustics, Vector and combined receivers, Interference

1. Introduction

It was discovered that field of acoustic intensity vector was vortical one (Shchurov V.A. et.al. 2010a, Shchurov V.A. et.al. 2010b, Shchurov V.A. et.al. 2011) when researching interference features of acoustic fields of noise-like signal from surficial source (ship) in the shallow sea wave-guide. Interference of acoustic pressure gives steady, almost determinate structure of acoustic energy distribution in vertical plane in the shallow sea wave-guide. Random component of acoustic field is generated by surface roughness and uneven sea bottom, also, by fluctuations of sound velocity associated with different processes in the wave-guide.

In the paper presented the organized order of vector features of acoustic fields in the vertical plane and vorticity of the field of acoustic intensity vector related to this order are considered. To our knowledge, the moving in acoustic wave is a potential and the vector field of oscillatory particle velocity of medium is also non-vortical. However, the field of vector of energy flux density (acoustic intensity vector) is vortical one. Fundamentality of the mentioned phenomenon is expounded by the next equation – $\mathrm{rot}(p\vec{V}^*) \neq 0$, namely:

$$\mathrm{rot}(p\vec{V}^*) = p\,\mathrm{rot}\vec{V}^* + [\mathrm{grad}p \times \vec{V}^*] = [\mathrm{grad}p \times \vec{V}^*], \quad \mathrm{rot}\vec{V}^* = 0. \tag{1}$$

proportion (1) was brought to:

$$\begin{aligned} \mathrm{rot}(p\vec{V}^*) &= -2\omega\rho_0[\mathrm{Re}\,\vec{V}\times\mathrm{Im}\,\vec{V}] = \\ -2\omega\rho_0\left[V_yV_z\sin(\varphi_y-\varphi_z)\vec{i}+V_xV_z\sin(\varphi_x-\varphi_z)\vec{j}+V_yV_x\sin(\varphi_y-\varphi_x)\vec{k}\right] &= \\ = -2\omega\rho_0\left(\mathrm{rot}_x p\vec{V}^*+\mathrm{rot}_y p\vec{V}^*+\mathrm{rot}_z p\vec{V}^*\right), & \end{aligned} \tag{2}$$

where p – acoustic pressure, $\vec{V}^*$ – complex-conjugate magnitude of oscillatory particle velocity vector, ω – circular frequency, ρ_0– unperturbed magnitude of medium density, V_i – amplitude value of particle velocity, (i = x, y, z); $(\varphi_y-\varphi_z)(\varphi_x-\varphi_z)(\varphi_y-\varphi_x)$ – phase's difference between components of oscillatory particle velocity.

Expression (2) is true in average, also for random stationary tonal signal. Mechanism of formation of vortex with horizontal components curl $\mathrm{rot_x}(p\vec{V}^*)\neq 0$ and $\mathrm{rot_y}(p\vec{V}^*)\neq 0$ can be explained in the following way. Let's this summary energy real flux from two sources of one frequency separate into its constituents from every wave of azimuth reference z (Shchurov V.A. 2006):

$$I_z = p_1V_1\cos\theta_1 + p_2V_2\cos\theta_2 + [p_1V_2\cos\theta_2 + p_2V_1\cos\theta_1]\cos(\varphi_2-\varphi_1)\,, \tag{3}$$

where p_1, p_2, V_1, V_2 - amplitudes of mono-chromatic signals of pressure and oscillatory particle velocity respectively; θ_1, θ_2 - angles between fluxes direction and axis z; $(\varphi_2-\varphi_1)$ – phase's difference between acoustic pressures of two waves. The first and the second items in (3) are z-components of every flux of energy under the absent other fluxes. The third item gives additional energy flux along z-axis, when both waves exist simultaneously. Expression (3) depends on the area size through which energy flux runs. If the linear area size was great in comparison to the wavelength, then, $<\cos(\varphi_2-\varphi_1)>=0$. If the linear area size was commensurable or less than the wavelength, then, at the given scale of distances $<\cos(\varphi_2-\varphi_1)>\neq 0$ another than zero, third item would change its sign, that results in alteration of direction in energy propagation in the expression (3). Thus, the energy running through the area towards +z will be returning into another point of this area towards –z. This points to the acoustic energy being propagated along closed contour, to generate a vortex.

Existence of vortices in the field of acoustic intensity was predicted theoretically in the 80-es of last century (Mann J.A. et.al. 1987), but actually the vortices of acoustic intensity in marine environment were discovered only at present time during experiment in the shallow sea (Shchurov V.A. et.al. 2010a, Shchurov V.A. et.al. 2010b, Shchurov V.A. et.al. 2011) in 2008.

It became possible due to design achievements in measuring vector-phase systems of hi-tech level and more modern algorithms of processing of experimental data (Shchurov V.A. 2006). A number of targeted experiments was fulfilled in Peter the Great Bay of the Sea of Japan in 2008-2010 over various depth of sites from 30 m to 250 m. Disclosed features of the interferential acoustic field were meeting conditions of existence of the vortices structures (Mann J.A. et.al. 1987). The same explorations performed in the deep ocean (in the nearest zone of illumination and at 500 m depth for measurements) with a tonal source dragged along 50 m depth and with the noise-like signals from vessels demonstrated that the formation of vortices structures of intensity vector was not recorded (Shchurov V.A. et.al. 2008, Shchurov V.A. et.al. 2010c). The presented work embraced research of the experimental work results and their statistical analysis according to identification of vortex features of acoustic intensity.

2. Method and Experiment Conditions

In the presented paper we shall give results of one experimental work having been in 2008. The research was performed using the combined systems over 5-1000 Hz frequency band. Technique of combined vectorial measurements and data processing were described in (Shchurov V.A. 2006). Measurements of oscillatory particle velocity of medium were fulfilled applying the electro-dynamic receiver of oscillatory velocity. The combined receiver was placed in the measuring cigar-shaped module being streamlined and possessing neutral floatage positioned at 70 m depth, at the site depth of 120 m. The axes x and y of the combined receiver were directed in horizontal plane. Axis z was vertical and directed from surface to bottom.

The slowly moving vessel of large-capacity that was navigating with constant 1.5 m/s speed was used as wideband source. The vessel passed by receiving system at traverse distance ~1000 m and moved away along a direct line from the receiving system to ~6000 m. All the vessel travel lay in the shallow sea part. The site depth above which this vessel traveled was equal to 100-200 m. The bottom there was a smooth flatness being a little

slope to the side of abyss frontier. Thus, the experiment conditions respond to the shallow sea parameters. Wave-guides of the shallow sea imply in itself such environment where a bottom type plays significant part in acoustic field formation. General contribution to the acoustic field formation in researched wave-guide was given by the refracted surficially rays being then reflected from bottom.

Time of research was October. The location coordinates are 131^0 17'48"E, 42^0 24'46"N. The sound velocity from depth: at surface was equal to1494.0 m/s; at 25 m depth –of 1486.1 m/s; at 50 m depth it was equal to1463.6 m/s; at 100m depth and on bottom it was of 1458.2 m/s. During experiment the speed of wind was changing within 5 – 7 m/s the fully developed roughness was observed.

3. The Results of Experiment

The results of statistical processing of experimental data are presented in fig. 1 – fig. 7. In fig. 1 there was compiled a sonogram of z-component of real part in the mutual spectrum $\mathrm{Re}\,S_{PV_z}(f,t)\cos\Delta\varphi_z$ that was observed under the solely moving vessel, where $\Delta\varphi_z(f,t)$ phases difference between acoustic pressure $p(t)$ and vertical component of oscillatory particle velocity $V_z(t)$. Averaging was exponential. Time of averaging was Δt = 2.9 s. Analysis band equaled Δf = 2.15 Hz. Frequency band was 5 – 800 Hz. At the moment of time t = 1500 s the traverse of a vessel passing by was observed. Fig. 1 exhibits high accuracy of the combined measuring system. If measuring module was unstable in water medium randomly changing its orientation and there was discovered the presence of vibration of a cowl shell and high pseudo-sound noises, then, interferential picture would not be contrast enough (Shchurov V.A. 2006). It is widely known that physical measurements based on the phase interferential measurements are the most accurate and under insignificant uncontrollable movements of receiving system this interferential picture in fig. 1 would be random.

In a black-and-white sonogram the black field means that the vertical z-component of energy flux density has direction from surface to bottom, the white field is congruent with contrary direction from the bottom to surface. It follows from fig. 1 that in the point of measurement the moving source creates interferential field where depending as on time, as on frequency, the vertical z-component of density vector of energy flux has constant feature periodically changing direction of propagation that was veering to 180°. Sonograms of horizontal components of energy flux density $\mathrm{Re}\,S_{PV_x}(f,t)\cos\Delta\varphi_x$ and $\mathrm{Re}\,S_{PV_y}(f,t)\cos\Delta\varphi_y$ aren't given in the work, because they don't possesses the same features and point to the steady transfer of acoustic energy in horizontal direction.

In fig. 2 there were presented acoustic characteristics for two frequencies $f_1 = 110$ Hz and $f_2 = 23$ Hz emitted by passing vessel. In fig. 2A and fig. 2C see module of spectrum density of acoustic pressure $S_{P^2}(f_{1,2},t)$; in fig. 2B and fig. 2D see z-component of real part of the mutual spectrum $\mathrm{Re}\,S_{PV_z}(f_{1,2},t)\cos\Delta\varphi_z$ depending on time and distance. Time t = 1500 s is congruent with position of traverse (distance till emitting source is ~1000 m); t = 5000 s is congruent with distance of ~6000 m. Interference nature of $S_{P^2}(f_{1,2},t)$ dependence on distance is usual in shallow sea. Due to $\mathrm{Re}\,S_{PV_z}(f_{1,2},t)\cos\Delta\varphi_z$ changing sign, following symbols are adopted at fig. 2B and fig. 2D. Expression sign «+» dB corresponds to the energy flux density directed downward (to bottom); «-» dB responds to the energy movement directed from bottom to surface.

4. Discussion

There is the research of interferential field features at $f_1 = 110$ Hz frequency depending on time and (distance) under the following magnitudes sampling (fig. 3): A – spectrum density of acoustic pressure $S_{P^2}(f_1,t)$; B – phase difference $\Delta\varphi_z(f_1,t)$ of mutual spectrum $S_{PV_z}(f_1,t)$; C is z-component of real part of the mutual spectrum $\mathrm{Re}\,S_{PV_z}(f_1,t)\cos\Delta\varphi_z$ In fig. 4 the dependence of polar angle $\theta(f_1,t)$ of intensity vector $\vec{I}(f_1,t)$ was compiled. The chosen items respond to time span equaled 2100–2450 s in the fig.1 sonogram. This time corresponded to 1200–1725 m distance span between source and receiver. There was displayed presence of fundamental connection between presented in fig. 3 and fig. 4 parameters of acoustic field. Acoustic pressure (fig.3A) fluctuates as a result of multi-beam interference, as it should be expected in the case of shallow sea.

The depths of interference minima of the acoustic pressure relative to neighboring interference maxima reach values from -5 dB to -15 dB. We denote particular points as **a, b, c, d, e,** and **f** in which $S_{P^2}(f_1,t)$ reaches its relative minimum values. In the neighborhood of these points, the z component of the energy flux density $\mathrm{Re}\,S_{PV_z}(f_1,t)\cos\Delta\varphi_z$ changes its direction by $\pm 180^0$ (fig. 3c). At points **a, c, e,** the direction of the energy flux

changes from surface-to-bottom to bottom-to-surface. The phase difference $\Delta\varphi_z(f_1,t)$ in the neighborhood of points **a, c, e** experience a jump (fig. 3b) by an angle of approximately 180^0, which should happen when the motion of energy changes to the opposite direction (Shchurov V.A. 2006).

The orientation in the vertical plane of the energy flux density vector (intensity vector) $\vec{I}(f_1,t)$ is determined by polar angle $\theta(f_1,t)$. At points **a, c, e,** the intensity vector without peculiarities passes through a value of $\theta = 90^0$ (fig. 4). Note that at $\theta = 90^0$, the intensity vector $\vec{I}\left\{S_{PV_x}, S_{PV_y}, S_{PV_z}\right\}$ lies in the horizontal plane xoy; i.e., in the neighborhood of points **a, c, e,** the z-component of the energy flux is equal to zero $\mathrm{Re}\, S_{PV_z}(f_1,t)\cos\Delta\varphi_z = 0$.

At points **b, d, f,** a change in the directions of the energy of motion from bottom-to-surface to surface-to-bottom occurs. In the neighborhood of points **b, d, f,** the phase difference $\Delta\varphi_z(f_1,t) \approx 0^\circ$, which corresponds to the direction of the intensity vector coinciding with the z axis, since the energy flux in the surface-to-bottom direction. In the neighborhood of these points, angle $\theta(f_1,t)$ undergoes "breaking" (fig. 4). From fig. 4, it is clear that over the span of the entire realization, the intensity vector $\vec{I}(f_1,t)$ changes its direction relative to the horizontal plane. As well, with a change in the sign of $\mathrm{Re}\, S_{PV_z}(f_1,t)\cos\Delta\varphi_z$ from "+" to "-", vector $\vec{I}(f_1,t)$ rotates without singularities (continuously) (points **a, c, e**). With a change in the sign of $\mathrm{Re}\, S_{PV_z}(f_1,t)\cos\Delta\varphi_z$ from "-" to "+", a jump in $\theta(f_1,t)$ occurs and the vector $\vec{I}(f_1,t)$ changes its direction jump wise (points **b, d, f**). Our analysis on the basis of values $S_{P^2}(f_1,t)$, $\Delta\varphi_z(f_1,t)$, $\mathrm{Re}\, S_{PV_z}(f_1,t)\cos\Delta\varphi_z$, $\theta(f_1,t)$ shows that the relative interference minima of acoustic pressure $S_{P^2}(f_1,t)$ (points **a, b, c, d, e, f**) define the regions of the shallow-sea waveguide space in which, in the vertical plane of the waveguide, a stable structure of oppositely directed energy flux is established. As a result, in the shallow-sea waveguide, intensity vector vortices $\vec{I}(f_1,t)$ arise in the vertical plane, which were described in (Mann J.A. et.al. 1987).

Note that with a change in directions of $\mathrm{Re}\, S_{PV_z}(f_1,t)\cos\Delta\varphi_z$ in the neighborhood of points **b, d, e,** and **f**, fluctuations arise due to the zero value of $\mathrm{Re}\, S_{PV_z}(f_1,t)\cos\Delta\varphi_z$; at these points, minimum values of $S_{P^2}(f_1,t)$ are observed, the phase difference $\Delta\varphi_z(f_1,t)$ undergoes breaking, and fluctuations in $\mathbf{Im}\, S_{PV_z}(f_1,t)$ are observed near these points, this result is not included into this paper. The set of these conditions is characterization of the existence of the center of an intensity vortex.

It is of our interest to compare observed acoustic field properties at a frequency f_1 = 110 Hz and wave length of approximately ~ 13.6 m with the same at a frequency f_2 = 23 Hz and wave length ~ 65.2 m. The analysis band is Δf =1.08 Hz; the time of averaging is Δt = 4.6 s (fig. 5). The combined receiver is located at the distance of 50m from the bottom. It follows from the interference picture (fig. 2C and fig. 2D), that (in comparison with the fig. 2A, and fig. 2B) acoustic wave of the frequency of 23 Hz perceive bottom and surface roughness a more "even", than wave of the frequency of 110 Hz. It means that real wave-guide is more "ideal" for the frequency of 23 Hz than for the one of 110 Hz. Moreover, interferences of acoustic pressure do not differ on principle, but real parts of z-components differ on principle: acoustic energy at a frequency of 23 Hz "flows" (except points **a, b, c**) mostly from surface to bottom on this time interval of 2000 – 2600 s (fig. 5 and fig. 6). But, in the neighborhood of the points **a, b, c**, polar angle $\theta(f_2,t)$ riches the following values: for the point **a** of $+60^0$, for the point **b** of $+45^0$, for the point **c** of $+30^0$, i.e. values, which are higher than $\theta(f_1,t)$ at the frequency of 110 Hz (fig. 4). It could be explained by the fact that energy penetrates into the ground and, as result of refraction inside the ground, energy returns to the wave-guide as caustic (points **a, b, c**).

Using the data obtained from experiment, we calculated the vorticity of the intensity vector for both frequencies according to formula (2). We calculated the phase differences $(\varphi_y - \varphi_z)(\varphi_x - \varphi_z)(\varphi_y - \varphi_x)$ from the mutual spectra of the oscillatory particle velocity components $S_{V_yV_z}(f_{1,2},t)$, $S_{V_xV_z}(f_{1,2},t)$, $S_{V_yV_x}(f_{1,2},t)$. We calculated the normalized curl components of the intensity vector $\mathrm{rot}_x\vec{I}(f_{1,2},t)$, $\mathrm{rot}_y\vec{I}(f_{1,2},t)$, $\mathrm{rot}_z\vec{I}(f_{1,2},t)$ and constructed their probability density histograms. The accumulation time of histograms was equal to the realization length, 350 s for frequency f_1 and 650s for frequency f_2.

Fig. 7A, fig 7B and fig. 7C show the histograms of probability densities ρ_z, ρ_x, ρ_y for random normalized intensity vector curl components $\mathrm{rot}_z\vec{I}(f_1,t)$, $\mathrm{rot}_x\vec{I}(f_1,t)$, $\mathrm{rot}_y\vec{I}(f_1,t)$, respectively. The mean value of the curl z-component is small and equal $<\mathrm{rot}_z\vec{I}(f_1,t)>=-0.09$, with a standard deviation of $\sigma=\pm 0.24$, which corresponds to an interval of phase difference angles of $0^\circ-14^\circ<(\varphi_y-\varphi_x)<0^\circ+14^\circ$. A phase difference of $(\varphi_y-\varphi_x)=\pm 14^\circ$ should be considered as an experimental error. Thus, in the horizontal plane xoy, vortices do not exist in the field of the energy flow density vector (intensity vector) of a single source. In the vertical planes xoz and yoz, the histograms of ρ_x and ρ_y have a different shape of distribution in which the largest probability density corresponds to values of $\mathrm{rot}_x\vec{I}(f_1)\approx\pm 1$ and $\mathrm{rot}_y\vec{I}(f_1)\approx\pm 1$. We divide the interval (-1.0, +1.0) into three intervals: the central interval (-0.25, +0.25) and two boundary intervals (-1.0, -0.25); (+0.25, +1.0).

We find probabilities $P_{x,y}$ for each interval and for the sums $\sum P_{x,y}$ for boundary intervals only (table 1). From the Table 1 and Fig. 7, it follows that probabilities P_x and P_y of vorticities in the boundary intervals significantly exceed the probability density of the central interval. The value of total probability $\sum P_{x,y}$ for each of the curl components is close to unity. Quantities $\mathrm{rot}_x\vec{I}(f_1)=\pm 1$ and $\mathrm{rot}_y\vec{I}(f_1)=\pm 1$ point to the existence of vortices of opposite directivity.

Fig. 7D, fig 7E and fig. 7F show the histograms of probability densities ρ_z, ρ_x, ρ_y for random normalized intensity vector curl components $\mathrm{rot}_z\vec{I}(f_2,t)$, $\mathrm{rot}_x\vec{I}(f_2,t)$, $\mathrm{rot}_y\vec{I}(f_2,t)$, respectively. Histograms for the frequency of 23 Hz are similar to the ones for the frequency of 110 Hz, but have some new features also. The vertical z-component of the curl has the mean value of $<\mathrm{rot}_z\vec{I}(f_2)>=-0.26$, with standard deviation of $\sigma=\pm 0.40$. Therefore, there is vorticity at frequency of 23 Hz in the horizontal plane. The phase differences between components of the oscillatory particle velocity, V_x and V_y, could lie inside the interval of angles of $-38^\circ<(\varphi_y-\varphi_x)<+14^\circ$, i.e. the shift of the phase difference to the negative angles is clearly higher than the error of the experiment. Maximum values of probability for x- and y- components of the curl lie in the neighborhood of the values $\mathrm{rot}_x I(f_2)=-1$ and $\mathrm{rot}_y I(f_2)=-1$. It indicates existence of the vortices of the negative direction only. The values of probabilities $\sum P_{x,y}$ are close to the unity for $\mathrm{rot}_x I(f_2)=-1$ and $\mathrm{rot}_y I(f_2)=-1$ (Table. 1).

Similar results were obtained in the other experiment for the depth of 30 m and frequency of 33 Hz in 2010. It is possible to connect the non-zero vorticity in the horizontal plane, $\mathrm{rot}_z\vec{I}(f_2,t)\neq 0$, with horizontal refraction of low-frequency sound.

As noted above, there is no vorticity peculiarity of the acoustic intensity vector in deep open ocean in near-field radiation zone in interference field of Lloyd mirror. It may be explained by the following. The interference in the Lloyd mirror occurs in co-directed rays, there are no energy flows with opposite directions (Shchurov V.A. et.al. 2008, Shchurov V.A. et.al. 2010c).

5. Conclusions

This paper presents the study of the mutual scalar and vector characteristics of the acoustic field of the single source on shallow sea for different distances between the source and combined receiver in the low – frequency band. Established vortex character of the field of vector of acoustic intensity does not contradict existing theory.

The comparison of vorticities of the field of intensity vector at frequencies of 23 Hz and 110 Hz shows, that a vortex character of energy transfer in shallow sea depends on acoustic wave frequency (length). Statistical analysis has shown that at frequency of 110 Hz in the vertical plane passing through the source and receiver, the normalized acoustic intensity vector curl values have horizontal x- and y-components differing from zero. The mean value of the vertical z-component of the curl is equal to zero in the limits of the experimental error.

At frequency of 23 Hz all three components of the normalized curl are not equal to zero. Besides, x- and y-

components of the curl have values close to the -1, i.e. there is vorticity of one sign, which is negative sign only. The mean value of the histogram of the vertical z-component of curl is not equal to zero. This fact shows the possibility of existence in the horizontal plane of the vorticity differing from zero.

It is the most probable that the origin of this vorticity is related to the horizontal refraction. The vortex properties of the energy "flow" in the vertical plane were observed under a continuous change in distance from 1000 m to 6000 m between the source and receiver. This physical phenomenon has a universal character and should be taken into consideration in solving fundamental and applied problems of underwater acoustics.

References

Mann J.A., Tichy J., Romano A.J. (1987). Instantaneous and time-averaged energy transfer in acoustics fields. *The Journal of the Acoustical Society of America,* 82, (4), 17-30. http://dx.doi.org/10.1121/1.395562

Shchurov V.A. (2006). *Vector acoustics of the ocean*. Vladivostok: Dalnauka, 296. (in English)

Shchurov V.A., Kuleshov V.P., Tkachenko E.S. (2010a). The phase spectra of interferential wideband surface source at shallow sea. *Collection of abstracts of the XXII session of Russian Acoustic Society and Session of the Scientific Counsel of the Russian Academy of Sciences on acoustics*. Moscow: GEOS, 2, 248-251.

Shchurov V.A., Kuleshov V.P., Tkachenko E.S. (2010b). The vortices of acoustic intensity in shallow sea. *Technical acoustics*. http: // ejta.org, 12.

Shchurov V.A., Kouleshov V.P., Tkachenko E.S., Ivanov E.N. (2010c). Features Determining Compensation of Counter Energy Flows in Acoustic Fields of the Ocean. *Acoustical Physics*, 56, (6) 1089–1096. http://dx.doi.org/10.1134/S1063771010060357

Shchurov V.A., Kuleshov V.P., Tkachenko E.S., Cherkasov A.V. (2011). The vortex transfer of acoustic energy at shallow sea. *The Acoustics of the ocean: Presentations of the XIII school - seminar named after academician L.B. Brehovskih and XXIII Session, Russian Acoustic Society*. Moscow: GEOS 94- 97.

Shchurov V.A, Lyashkov A.S., Tkachenko E.S. (2008). Statistical Characteristics of the Dynamic Noise Energy Flux in the Ocean in the 400 to 700 Hz Frequency Band. *Acoustical Physics*, 54, (4), 518–525. http://dx.doi.org/10.1134/S106377100804012X

Table 1. Probabilities of vorticity by intervals

Interval	P_x 110 Hz	P_y 110 Hz	P_x 23 Hz	P_y 23 Hz
-0.25, ÷ +0.25	0.21	0.15	0.09	0.08
-1.0, ÷ -0.25	0.47	0.50	0.82	0.84
+0.25, ÷ +1.0	0.32	0.35	0.09	0.08
$\sum P_{x,y}$	0.79	0.85	0.91	0.92

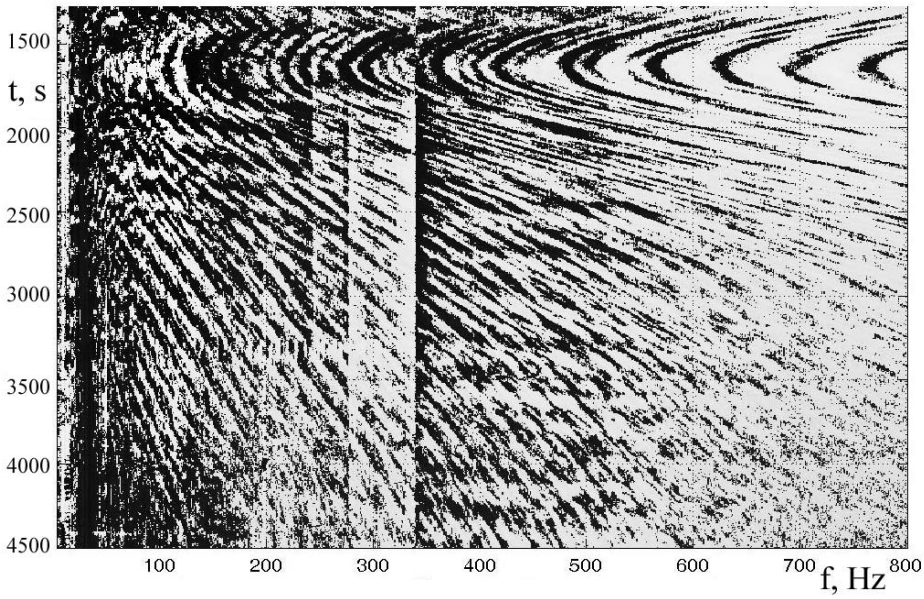

Figure 1. Sonogram of real part in the mutual spectrum of acoustic pressure and z-component of oscillatory particle velocity $\mathrm{Re}\, S_{PV_z}(f,t)\cos\Delta\varphi_z$.

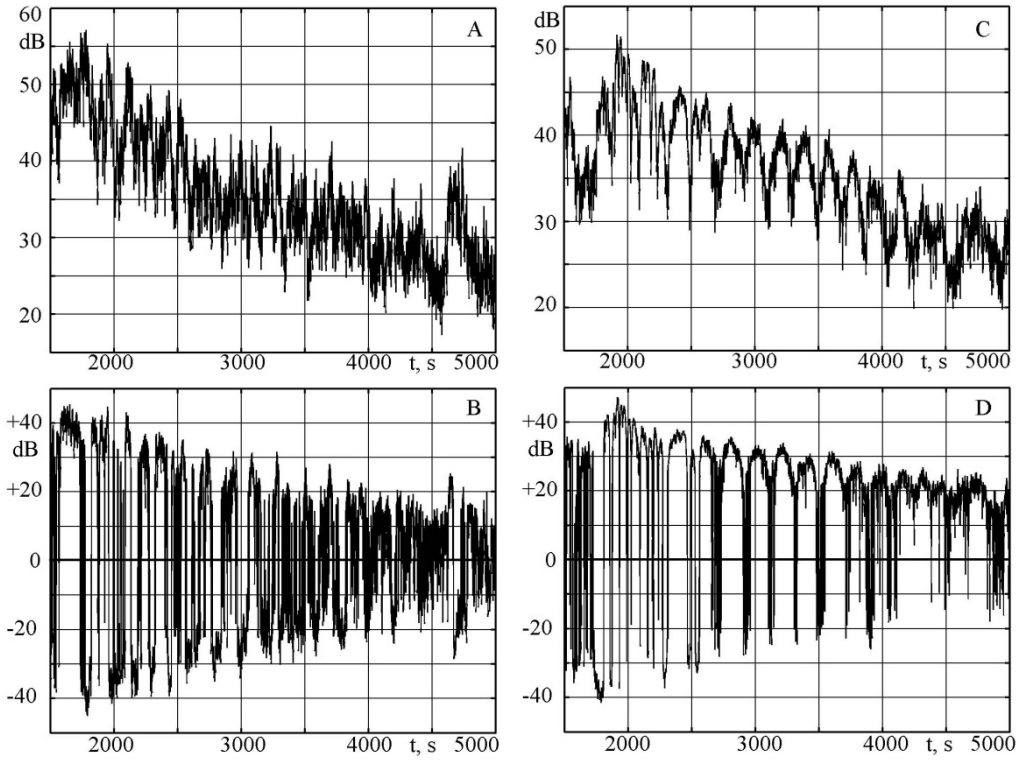

Figure 2. Dependence on time (distance): A – $S_{P^2}(f_1,t)$ spectrum density of acoustic pressure; B – $\mathrm{Re}\, S_{PV_z}(f_1,t)\cos\Delta\varphi_z$ spectrum density of z-component of acoustic intensity; $f_1 = 110$ Hz, analysis band equaled Δf = 2.15 Hz, time of averaging was Δt = 2.9 s. C – $S_{P^2}(f_2,t)$ is spectrum density of acoustic pressure; D – $\mathrm{Re}\, S_{PV_z}(f_2,t)\cos\Delta\varphi_z$ spectrum density of z-component of acoustic intensity; $f_2 = 23$ Hz, analysis band equaled Δf = 1 Hz, time of averaging was Δt = 5 s.

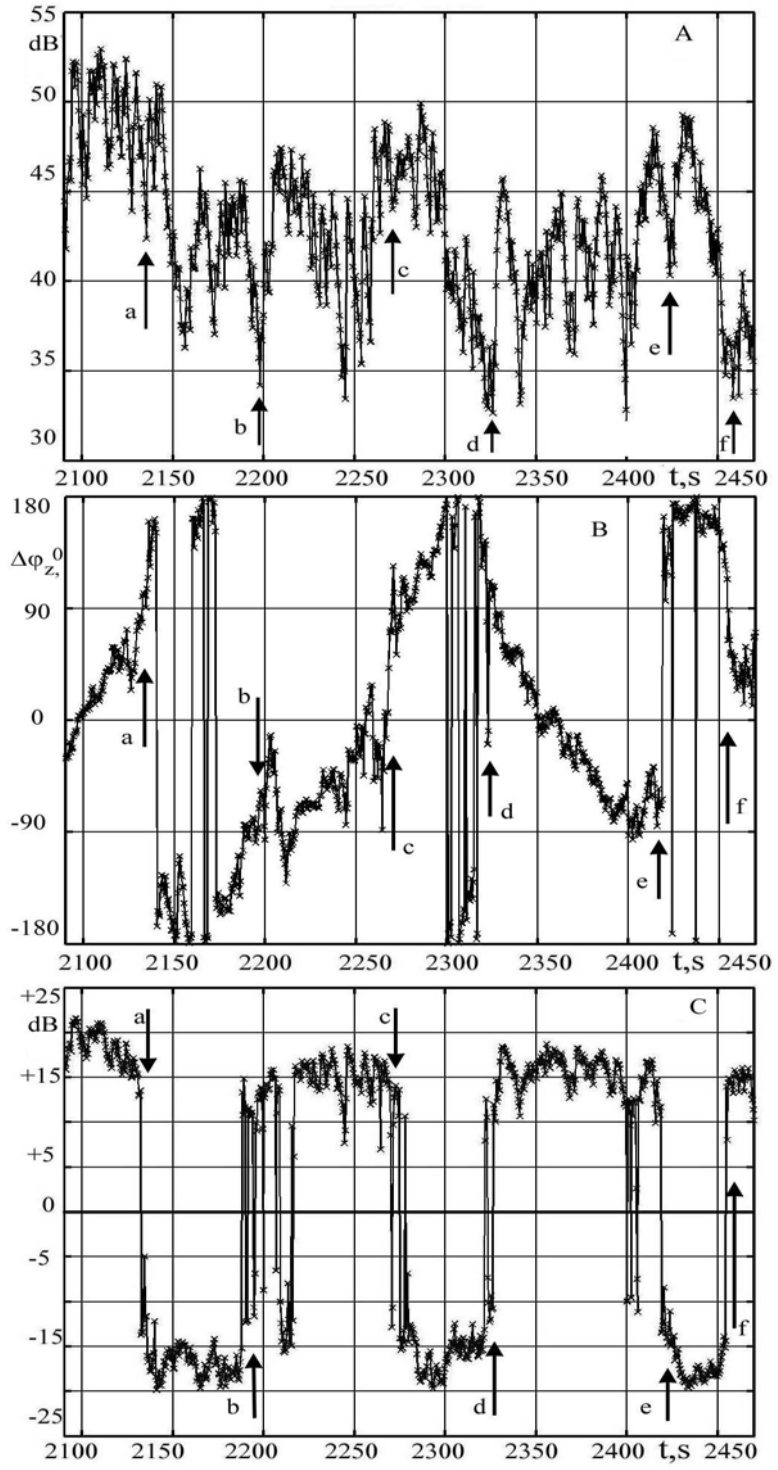

Figure 3. Dependence on time (distance): A – $S_{p^2}(f_1,t)$ spectrum density of acoustic pressure; B- phase difference $\Delta\varphi_z(f_1,t)$ between acoustic pressure and z-component of oscillatory particle velocity; C – $\mathrm{Re}\,S_{PV_z}(f_1,t)\cos\Delta\varphi_z$ – z-component of acoustic intensity; $f_1 = 110$ Hz. Averaging was exponential, analysis band equaled $\Delta f = 2.15$ Hz, time of averaging was $\Delta t = 2.9$ s.

 ISSN 1916-9639 E-ISSN 1916-9647

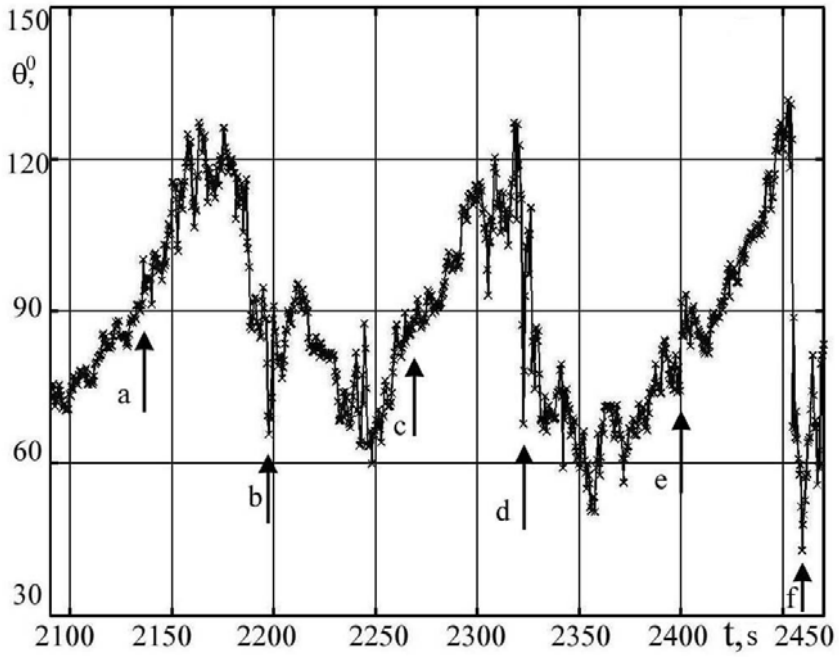

Figure 4. $\theta(f_1,t)$ – polar angle of the intensity vector $\vec{I}(f_1,t)$ vs time (distance).

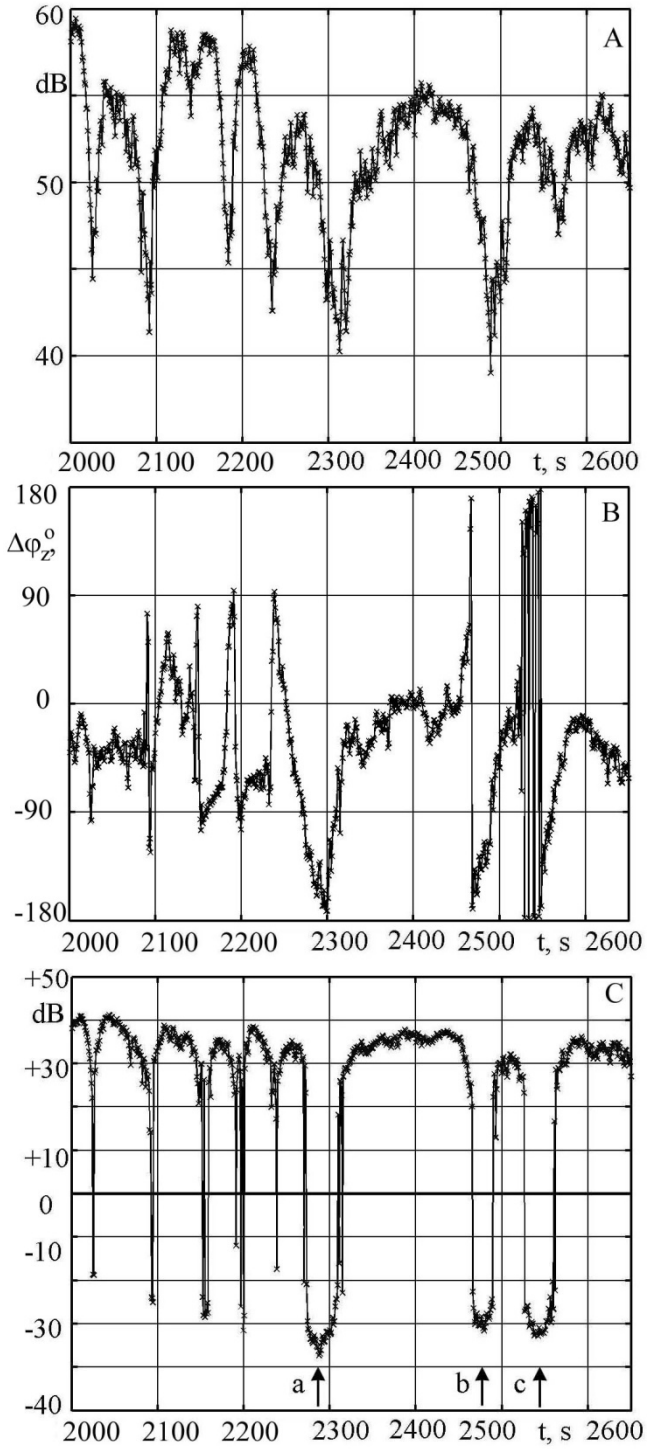

Figure 5. Time dependence (or distance dependence): A – $S_{P^2}(f_2,t)$; B – $\Delta\varphi_z(f_2,t)$; C – $\mathrm{Re}\, S_{PV_z}(f_2,t)\cos\Delta\varphi_z$, f_2 = 23 Hz, Δf=1.08 Hz, Δt = 4.6 s.

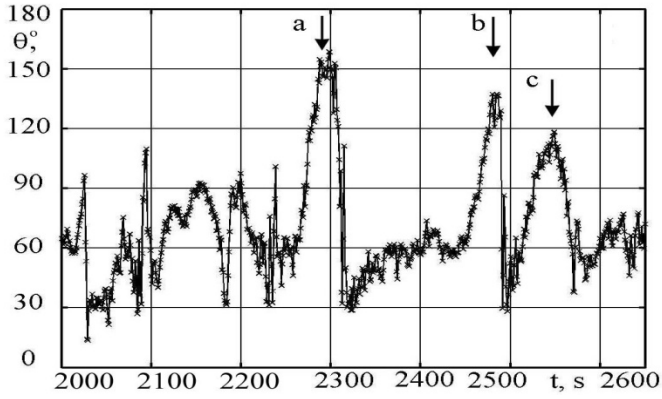

Figure 6. Polar angle $\theta(f_2,t)$ of the intensity vector vs time (distance).

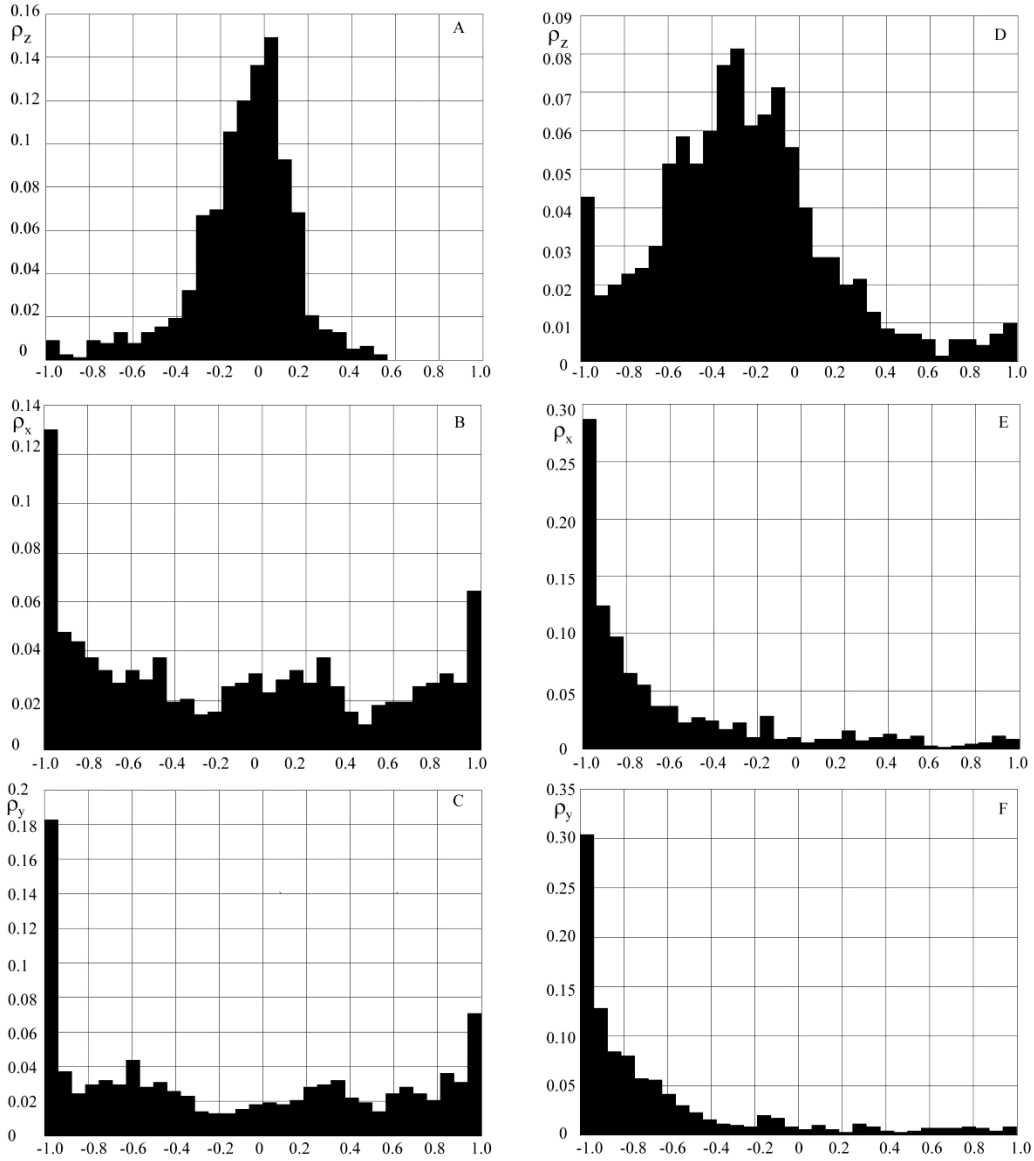

Figure 7. Histograms of the probability densities ρ_z, ρ_x, ρ_y of the normalized values of random variables: A, D – $\mathrm{rot}_z \vec{I}(f_{1,2})$; B, E – $\mathrm{rot}_x \vec{I}(f_{1,2})$, C, F – $\mathrm{rot}_y \vec{I}(f_{1,2})$. Accumulating time for the histograms is 350 s for f_1, is 650 s for f_2.